Chalcogenide glasses and structures for quantum sensing

S. K. Sundaram[1], B. R. Johnson, M. J. Schweiger, J. E. Martinez, B. J. Riley,
L. V. Saraf, N. C. Anheier, Jr., P. J. Allen, J. F. Schultz
Pacific Northwest National Laboratory, Richland, WA 99352-0999

ABSTRACT

Chalcogenide glasses are formed by combining chalcogen elements with IV-V elements. Among the family of glasses, As_2S_3, and As_2Se_3 are important infrared (IR) transparent materials for a variety of applications such as IR sensors, waveguides, and photonic crystals. With the promise of accessibility to any wavelengths between 3.5 and 16 μm using tunable quantum cascade lasers (QCL) and chalcogenides with IR properties that can be compositionally adjusted, ultra-sensitive, solid-state, photonic-based chemical sensing in mid-wave IR region is now possible. Pacific Northwest National Laboratory (PNNL) has been developing quantum cascade lasers (QCLs), chalcogenides, and all other components for an integrated approach to chemical sensing. Significant progress has been made in glass formation and fabrication of different structures at PNNL. Three different glass-forming systems, As-S, As-S-Se, and As-S-Ag have been examined for this application. Purification of constituents from contaminants and thermal history are two major issues in obtaining defect-free glasses. We have shown how the optical properties can be systematically modified by changing the chemistry in As-S-Se system. Different fabrication techniques need to be employed for different geometries and structures. We have successfully fabricated periodic arrays and straight waveguides using laser-writing and characterized the structures. Wet-chemical lithography has been extended to chalcogenides and challenges identified. We have also demonstrated holographic recording or diffraction gratings in chalcogenides.

Key words: Chalcogenide, glass formation, microstructure, laser writing, lithography, holography

1. INTRODUCTION

Integrated IR photonic devices require waveguide structures to efficiently transport IR light between various components. Chalcogenide glasses are excellent candidate materials for IR waveguides due to their relatively high transparency from ~ 2 – 12 μm. Chalcogenide glasses are amorphous materials containing one of the chalcogen elements (e.g. S, Se, Te) and can contain a wide array of other elements (e.g. As, Ge, Cd, etc.). Within this family of materials, arsenic trisulfide, As_2S_3, is one of the most studied and well known chalcogenide glasses.[1,2] As_2S_3 has excellent IR transparency and there are extensive literature references about its use as a waveguide material and as a fiber.[3-16] It is also a photo-modifiable material, that is, its optical properties, such as the index of refraction, can be altered by exposing it to light near its absorption band edge.[17-24] As a consequence, it is a relatively straight forward and direct process to create waveguides in As_2S_3 by laser-writing. In the case of As_2S_3, the writing can be done with a standard HeNe laser, which is readily available. Laser writing is a very flexible technique since the size, shape, and pattern of the structures to be written can be easily changed, including curved structures. Laser-written structures can also be created below the surface within the glass (buried structures). This provides a built-in cladding and protection for the waveguides. Additionally, 3D structures may also be possible. In addition to laser-writing, lithography can also be applied to fabricate structures, especially ribbed wave guides. Chemical wet lithography facilitates mass production. Since it is transparent in the visible range, it is easier to locate and characterize laser written structures in As_2S_3 than in some other chalcogenide glasses that are opaque in the visible (e.g. As_2Se_3). High non-linear optical properties of As_2S_3 glass makes it a good candidate for use in active photonic devices such as switches, modulators.[1, 25-30] Having both passive (waveguide) and active (modulators) components made from the same material is very appealing for integration of various optical components. We have formed over 13 different glass compositions in bulk as well as in thin film forms. We present our results on processing of chalcogenide glasses and fabrication of various structures for quantum sensing.

[1] sk.sundaram@pnl.gov; phone 509-373-6665; fax 509-376-3106; Pacific Northwest National Laboratory, P. O. Box 999, MSIN K6-24, Richland, WA 99352.

2. CHALCOGENIDE GLASS SYSTEMS

Our glass fabrication efforts were focused on the As-S binary, and the As-S-Se, and on the As-S-Ag ternary systems. Table 2.1 shows the compositions prepared in this project. Five different binary As-S glasses were made in addition to four ternary As-S-Se glasses and $As_{40}Se_{60}$. Figure 2.1 shows a ternary As-S-Se diagram with glass samples from these compositions super-imposed on it ($As_{24}S_{38}Se_{38}$ not pictured). These compositions were chosen so as to determine composition-property trends within this ternary system. Additionally, three different glasses were made in the As-S-Ag system (Table 2.1) in support of our photolithography effort. The compositions chosen were based on reports in the literature regarding lithography based photo-dissolution of silver into arsenic trisulfide,[1-6] as well as glass forming studies in the As-S-Ag ternary system.[6-7]

Table 2.1. Target glass compositions synthesized

As-S system	As-Se and As-S-Se systems	As-S-Ag system
$As_{30}S_{70}$	$As_{40}Se_{60}$	$As_{28}S_{57}Ag_{15}$
$As_{33}S_{67}$	$As_{40}S_{40}Se_{20}$	$As_{25}S_{50}Ag_{25}$
$As_{35}S_{65}$	$As_{40}S_{30}Se_{30}$	$As_{27}S_{41}Ag_{32}$
$As_{40}S_{60}$	$As_{40}S_{20}Se_{40}$	
$As_{45}S_{55}$	$As_{24}S_{38}Se_{38}$	

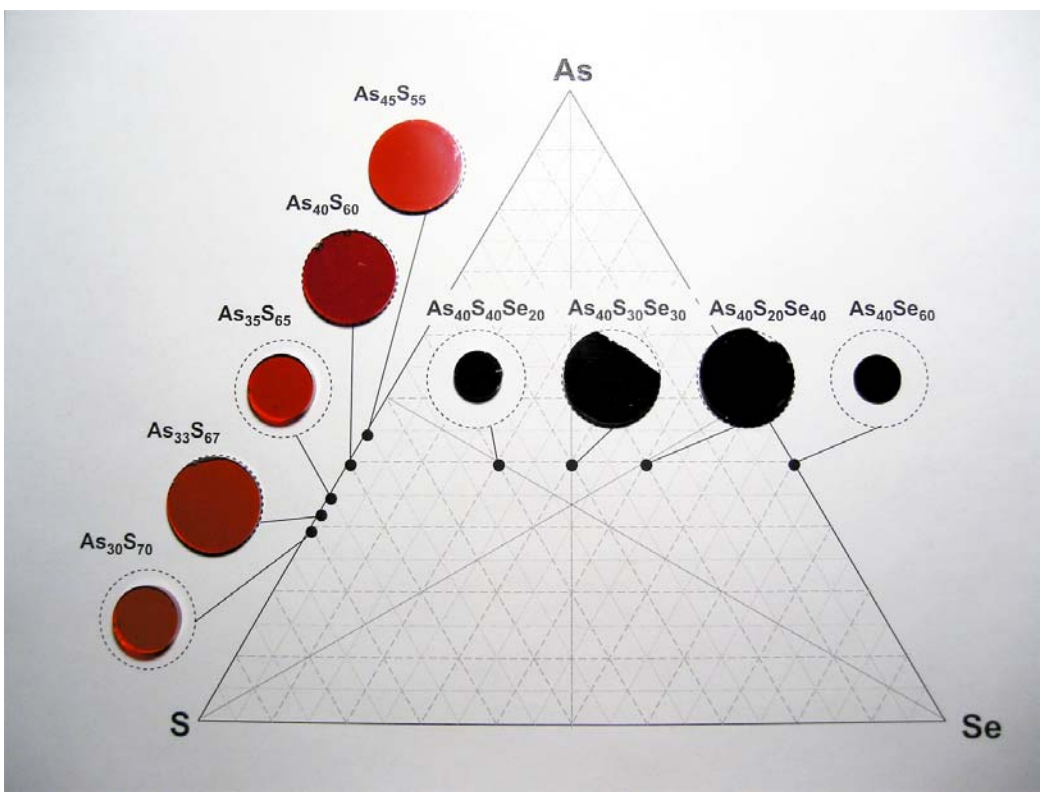

Figure 2.1. Ternary diagram showing the various As-S-Se chalcogenide glasses synthesized at PNNL

A comparison of FTIR transmission spectra for five chalcogenide glass compositions along the As_2S_3 - As_2Se_3 binary join (the horizontal line connecting As_2S_3 and As_2Se_3 shown in Figure 2.1) is shown in Figure 2.2. The objective was to determine the effects of composition on IR transparency within the 8 – 12 µm window. A similar study was done with the five glasses made in the As - S binary system (Table 2.1), and As_2S_3 was identified as having suitable transparency between 8 – 12µm. Basic statistical data was collected from the transmission spectra within the window, and the results are summarized. Major observations from the data are:

- With increasing Se content, the transmission spectra become more uniform and horizontal between 8-12 µm.
- Most of the absorption losses below 8 µm can be attributed to impurities from the source chemicals used for sulfur.
- The two most transparent glasses from 8-12 µm via. FTIR were $As_{40}S_{20}Se_{40}$, and $As_{40}Se_{60}$. Although arsenic triselenide has the flattest FTIR spectra, it cuts off rather sharply at 11.8 µm, while the two ternary glasses, $As_{40}S_{20}Se_{40}$, and $As_{40}S_{30}Se_{30}$ cut off more gradually, and are actually more transparent at even slightly higher wavelengths. If the absorption losses due to O_2 contamination can be resolved for these glasses, they may prove to be even more transparent from 8-12 µm than arsenic triselenide.

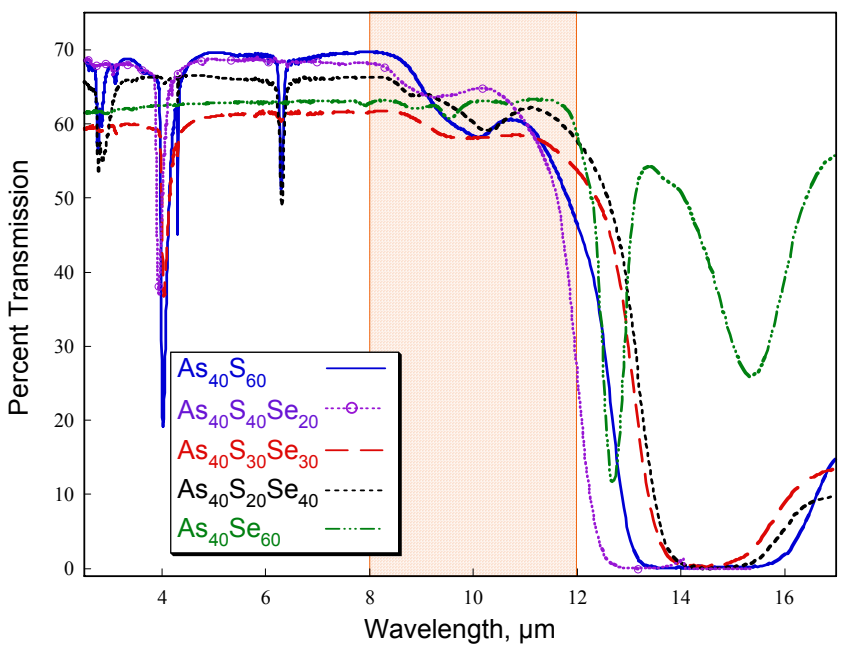

Figure 2.2. Comparison of FTIR transmission spectra for five different glasses in the As-S-Se ternary system. The spectral region of interest, 8-12 µm is highlighted. Two important features to standout: 1) Absorption peaks below 8 µm can be correlated to the sulfur-bearing glasses, since these peaks are not observed in $As_{40}Se_{60}$. 2) Within the 8-12 µm window, higher selenium content correlated to a "flatter" transmission spectrum. (Note: The percent transmission values are neither normalized nor corrected for differences specimen thickness. The values are accurate within ± 10% limit.)

3. STRUCTURES

3.1. Laser writing

Laser modification experiments were conducted with chalcogenide glasses of various compositions to determine the effects of composition on photomodification. The goal for successful MWIR waveguide structures is to embed them within the bulk of the glass. However, it was difficult to adequately characterize embedded structures. Therefore, photomodification experiments were done on the surface of the glass.

The $As_{40}S_{60}$ glasses were synthesized at PNNL using the ampoule, rocking-furnace method described elsewhere.[31-33] Sections were cut from the ampoule approximately 3 mm thick, and were polished to a sub-micron surface finish. The glass disks were photomodified using a HeNe laser at a wavelength of 632 nm, and at a power setting of 10 mW. For the first set of experiments, an array of spots was written on the specimens with a focused beam by exposing them for successively longer times. A second set of experiments was conducted by irradiating the specimens with a de-focused beam for very long times so as to create a large enough area to allow characterization with micro-Raman, micro FTIR, and energy dispersive spectroscopy (EDS). Arsenic trisulfide ($As_{40}S_{60}$) displayed photo-expansion distinctly in Figure 3.1. No significant loss of chemical homogeneity was observed, as shown in EDS dot mapping in Figure 3.2.

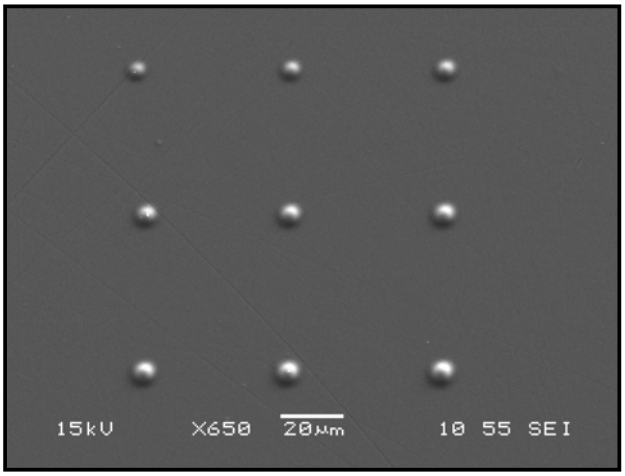

Figure 3.1. Photomodification of $As_{40}S_{60}$.

Micro-Raman spectroscopy was performed on the bulk as well as on the larger, photomodified spots to determine the effect of photomodification on chemical bonding. Raman spectroscopy is a technique that examines the inelastic scattered light from a material that has been illuminated by an intense light source, such as a laser. Various photon and phonon scattering events occur as the incident light interacts with the chemical bonds in the sample, and this causes shifts in the wavelength of the scattered light. Crystalline materials produce very sharp, well-defined shifts, since the bonds in an ordered crystalline material are very specific. In amorphous materials, there is a broad distribution of bond angles and energies, which subsequently produce broad, diffuse Raman spectra. Figure 3.3 shows a comparison of the Raman spectra from the bulk and from photomodified regions of $As_{40}S_{60}$. The photomodified spectra were broader and more diffuse than the bulk specimens. This provides valuable insight to aid understanding what happened to the material during photomodification: The sample was heated up by the laser (possibly above the glass transition temperature) and rapidly air quenched. This resulted in a more disordered material, probably less dense (hence photo-expansion) and thus the broader, more diffuse Raman spectra.[8-10] From these initial photomodification studies on As-S chalcogenide glasses, we conclude that the laser alters the chemical bonds of the glass, possibly due to a thermal effect by rapid heating and subsequent rapid cooling. This results in a more disordered material, that is most likely less-dense (photo-expansion) and with an altered index of refraction. In regards to creating embedded laser-written structures, the photo-expansion effect will induce increased strain within the material. The increase in strain may be deleterious to the integrity of the material. Additionally, depending on the coupling between changes in index of refraction (photodarkening) and photoexpansion, it is possible that the strain from the bulk that will limit photoexpansion may also limit photodarkening. In other words, a given laser fluence that would create a certain magnitude of a photo-induced effect on the surface, may not produce the same magnitude of an effect within the bulk. If the same magnitude of a photo-induce effect is created within the bulk as on the surface, the subsequently created strain may be deleterious to the integrity of the piece. Consequently, for embedded structures, it would appear preferable to find a material that has very low photoexpansion response in comparison to photodarkening for a given laser fluence.

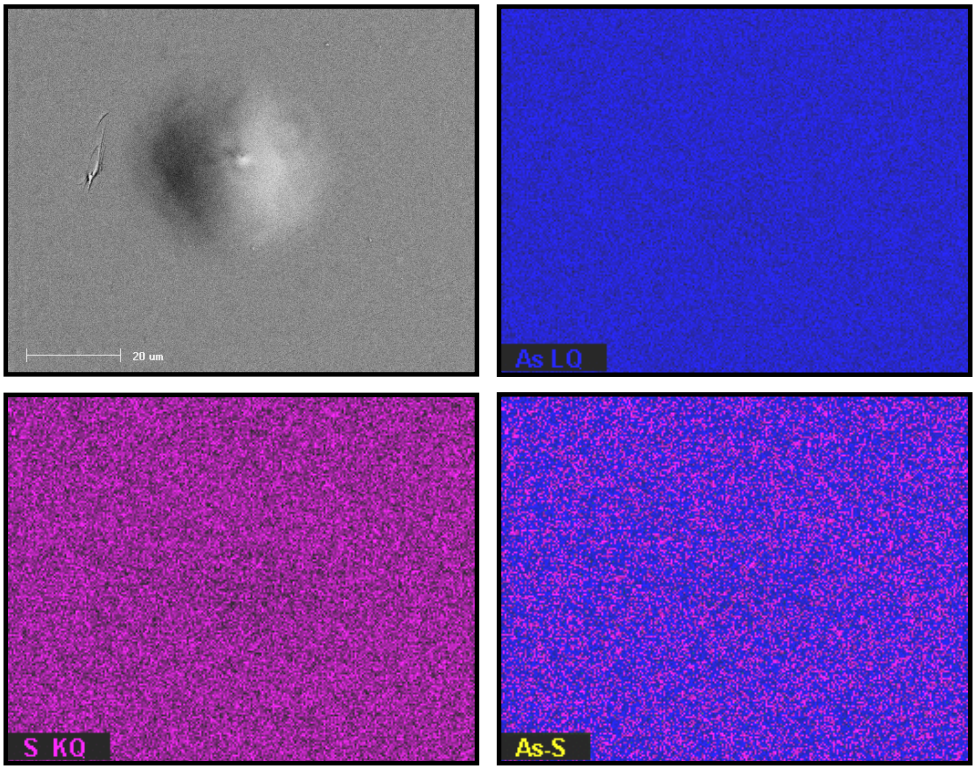

Figure 3.2. EDS dot mapping of a large diameter photomodified spot in $As_{40}S_{60}$ glass. The dot map shows the spatial distribution of the elements S and As, and the combined, overlay shows that the specimen was essentially homogeneous, and that there was not a significant re-distribution of the components due to photomodification.

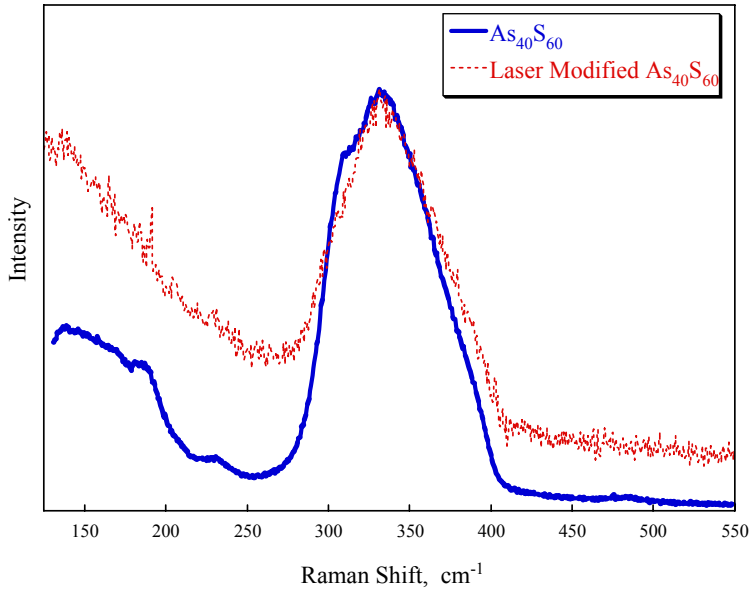

Figure 3.3. Raman spectra from bulk and photomodified $As_{40}S_{60}$

3.2. Lithography

In addition to novel direct laser writing in chalcogenide glass, experiments were done to develop photo-lithographic technology to support MWIR and LWIR photonic device needs. Traditional photolithography technology as applied to the silicon and semiconductor industries is focused on creating ever smaller and smaller structures. Currently, the industry standard is approaching 157 nm resolution. However, for photonically active optical circuits, the minimum feature size is dictated by the wavelength of light being propagated. Generally, for high performance optical transmission, single mode waveguide structures are necessary. Computer modeling with Rsoft Beamprop™ was done to calculate the appropriate dimension for single mode waveguides in chalcogenide glass at MWIR wavelengths. Figure 3.4 shows a schematic of the model used for these calculations. The results specified that feature sizes about 30 – 40 µm were required for a 10-12 µm IR wavelength. The modeling results also demonstrated that very extremely tight control must be maintained on both feature dimensions as well as refractive index in order to obtain the maximum performance out of the structure. Unfortunately, the fabrication of feature sizes this length scale is extremely challenging. These length scales are too small (by approximately 1.5 – 2 orders of magnitude) for traditional machining approaches, yet are exceedingly large (approximately 2 – 3 orders of magnitude) for traditional thin film lithographic techniques. Consequently, this is a new, novel endeavor that encompasses many engineering, materials, and chemical processing challenges.

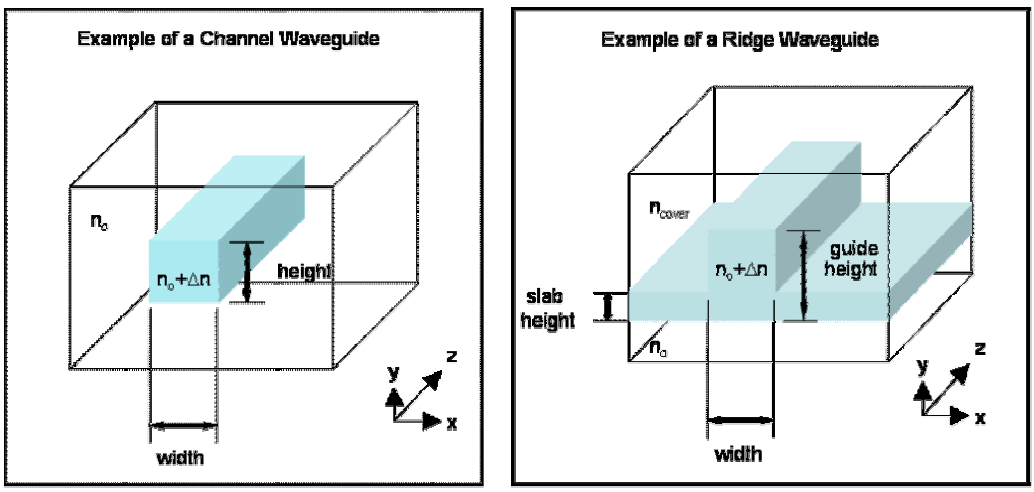

Figure 3.4. Schematic view of channel and ribbed waveguide structures modeled using computer software to determine appropriate feature sizes for single mode waveguides in chalcogenide glass.

Our objective was to explore the feasibility of applying and modifying standard lithographic technology to create photonic structures 20-40 µm in size. This problem was divided into three major tasks. The first task was to develop the ability to deposit thick films onto a substrate. The second task was to create suitable mask designs to build single mode, linear, ribbed, waveguide structures. The third task was to develop suitable etchant chemistry and etching protocol to create ribbed waveguides in the thick film. A structure was successfully fabricated with lines and spaces of 35 nm utilizing wet etching methods with a ratio of sodium hydroxide:isopropanol:distilled water (NaOH:IPA:DI) of 1:25:50.[34] It was unknown what concentration of NaOH was used by Kozicki and it was assumed that the ratios stated were by volume. From this prior knowledge, the concentration of NaOH chosen for these experiments was a 4 N, or 4 M, NaOH solution. The concentration of 4 M NaOH was altered while keeping the volume ratios of IPA and DI constant to determination to obtain a one variable etch rate curve of etch depth versus NaOH overall solution concentration (M). In performing chalcogenide glass etching using different mixtures of 4 M NaOH, isopropyl alcohol, and distilled water, some interesting results were obtained. In addition to the differences between the etchants, much variation was noticed in regards to the profilometry data gathered. If using the Si/SiO_2 technology mentioned previously, the step-height and orientation of the ribs left behind after selective etching were very uniform and consistent throughout the sample. When looking at Figure 3.5, a comparison between the Si/SiO_2 system and the chalcogenide glass system, many differences are seen. The sample shown for the Si/SiO_2 system (Figure 3.5-A, -C, and -E) was etched in BOE (Buffered-Oxide-Etch – an HF/NH_4F mixture), solution for 19 minutes revealing 0.7936 µm step height verified via optical profilometer (Figure

3.5-E). The sample shown for the chalcogenide glass etching system is the Sample B glass used in measuring the etch rate for the 1:5:10 etchant. Figure 3.5-F revealed a step-height of 0.7533 µm via optical profilometer, a similar step-height to Figure 3.5-E. As seen in the oblique plots, Figure 3.5-B, the surfaces on the chalcogenide sample are very rough and variable while the top surfaces on Figure 3.5-A are quite smooth and uniform. The smoother the top reference surface, the more accurate and precise is the measurement taken at that location.

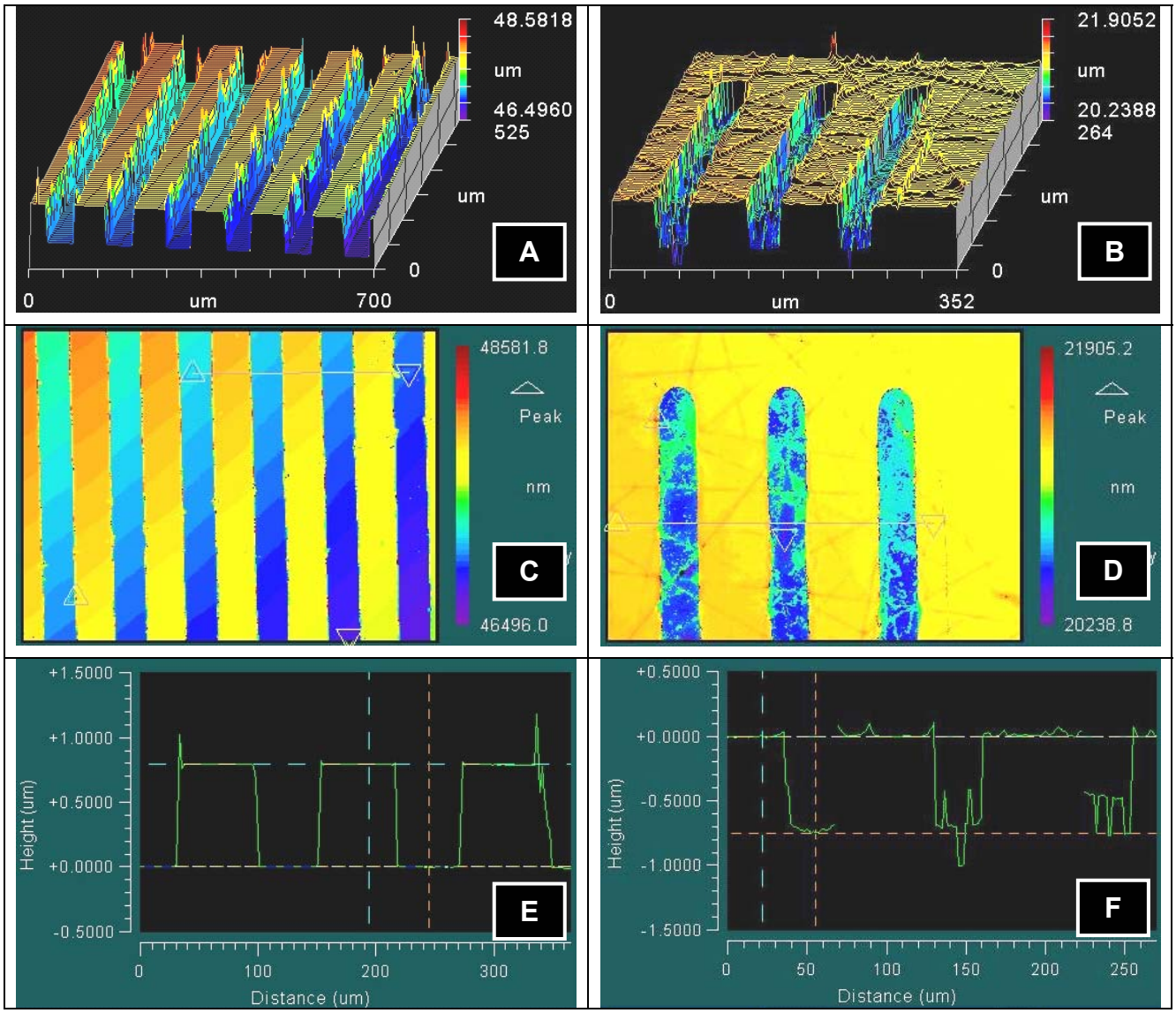

Figure 3.5. -A, -B, -C, -D, -E, and -F. Comparing optical profilometry of Si/SiO_2-etching system (A, C, E) with chalcogenide-etching system (B, D, F). Figure 3.5-A, -C, and –E show uniform, definite edges for measuring step-heights, whereas Figure 3.5-B, -D, and –F show extremely variable, rough, and nonuniform edges making step-height measurements difficult with any high degree of precision or accuracy.

When comparing top views Figure 3.5-D and Figure 3.5-C, the lower (bluer regions), are less well allocated. Figure 3.5-C shows a very uniform trench depth whereas when measuring the step-height for Figure 3.5-D, depending on where the measurements were taken, a high degree of variance would be observed. When comparing surface profiles, Figure 3.5-E displays very sharp, well-defined edges in peak structure whereas Figure 3.5-F shows not only very poor edges, the

depth of the etched trenches is quite difficult to measure so the only accurate way to measure the step-height with this sample is to take an averaged slice through the trench bottoms as was done. This was attributed to poor surface preparation. With better surface preparation, this was found to improve.

3.3. Holography

The goal of this investigation was to explore fabrication techniques of photonic bandgap structures produced in chalcogenide glass using holographic methods. This work will take advantage of PNNL's experience with the photomodification properties of chalcogenide glass, the availability of custom vacuum deposition systems, extensive experience fabricating and characterizing chalcogenide glasses, and novel holographic single step recording methods.

Experimental holographic recording techniques outlined in literature[35] were replicated using PNNL deposited thin chalcogenide thin films. Approximately 50 holographic diffraction gratings were recorded in As_2S_3, $As_{24}S_{38}Se_{38}$, and silver-doped chalcogenide glass films. During this study, we observed large variation in diffraction efficiencies as the exposure and film parameters were changed. Initial experiments were performed with As-S thin films of non-uniform thickness. To reduce variations in the deposited film thickness and improve the performance of the films, a rotary sample holder was designed, fabricated, and installed in PNNL's vacuum deposition system (Figure 3.6). Following the rotary sample holder installation, the film depositions demonstrated outstanding film thickness uniformity (Figure 3.7). Subsequent holographic exposures showed a significant improvement in repeatability.

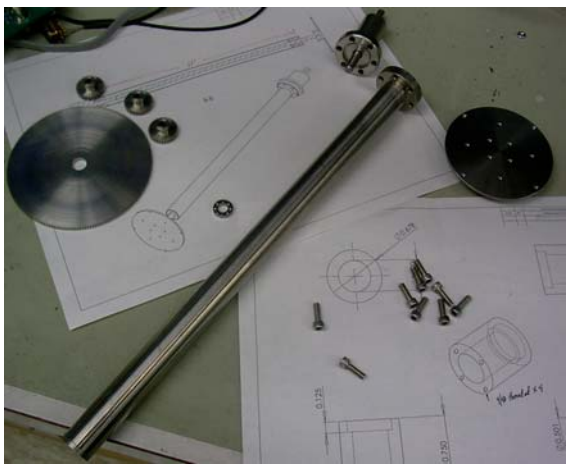

Figure 3.6. A rotary sample holder was designed and fabricated to improve the thin film thickness uniformity

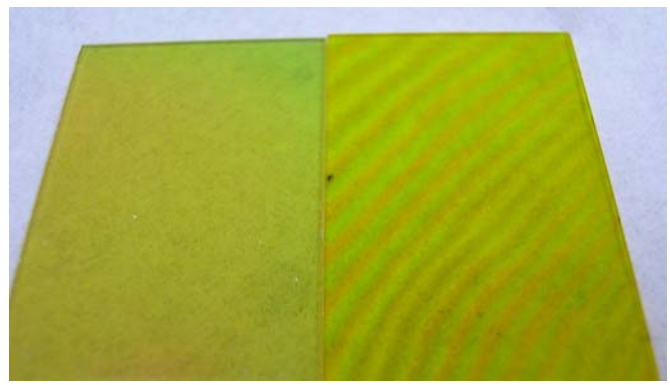

Figure 3.7. Chalcogenide glass thin films thickness uniformity improvement as evidenced by the visible interference fringes (Right: 2.25 µm film thickness variation, Left: < 0.1 µm variation)

It should be noted that these diffraction gratings are phase gratings, not relief gratings. Relief gratings could be created in chalcogenide glasses, due to its photoexpansion properties. However, these gratings are made in thin films, which create only nanometer scale relief structures. Phase gratings diffract light due to sinusoidal refractive index modulation in the glass. The modulations are recorded with the Lloyd's mirror interferometer (holography).

The refractive index modulation amplitude and the depth of the grating layer are critical parameters in the performance of the grating. Neglecting the glass intrinsic absorption, the diffraction efficiency is given by

$$\eta = \frac{I_1}{I_0} = \tan^2\left(\frac{\pi \Delta n d}{\lambda \cos\theta_i}\right)$$

where Δn is the index modulation, d is the phase grating thickness and θ_i is the incident angle. The direction of diffracted light is a function of the incident angle and the grating period according to the classical grating equation

$$\Lambda(\sin\theta_i + \sin\theta_m) = m\lambda$$

where Λ is the grating period and m = ± 0, 1, 2, … is the diffracted order number. If the grating illumination satisfies the Bragg condition,

$$\sin\theta_i = \lambda / 2n\Lambda$$

where n is the average refractive index of the glass in the grating region, then diffraction efficiencies approaching 100% are possible. High efficiency over moderately broad angular and spectral bandwidths can be achieved, but peak efficiency is usually decreased with increased bandwidth. The proper laser power densities and exposure times were established for 514 nm argon-ion laser illumination. The optimum parameters were determined by measuring the diffraction efficiencies of the diffraction gratings.

Holography experiments were performed using thin films (2 µm thick) of As_2S_3 deposited onto glass slides and holographically patterned using an argon-ion laser. Diffraction gratings with periodicities from 0.7 to 12.5 microns and film thickness from 0.2 to 8.0 microns with a 3 µm lateral resolution were fabricated and characterized. The holographic diffraction gratings were examined with a non-contact optical profilometer and an SEM. The grating structure revealed a uniform periodic structure with little or no distortion (Figure 3.8 and 3.9).

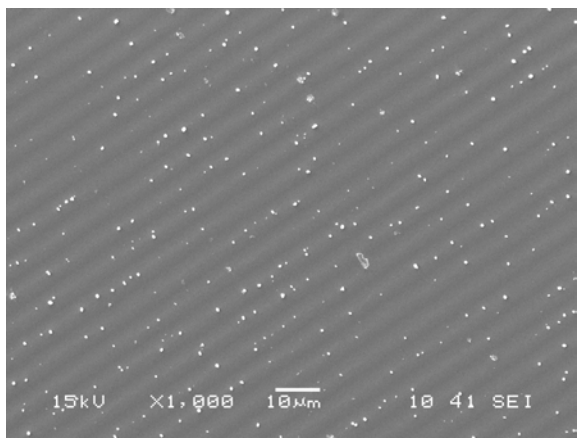

Figure 3.8. A SEM image showing a holographic grating structure with a grating period of ~ 5.5 µm

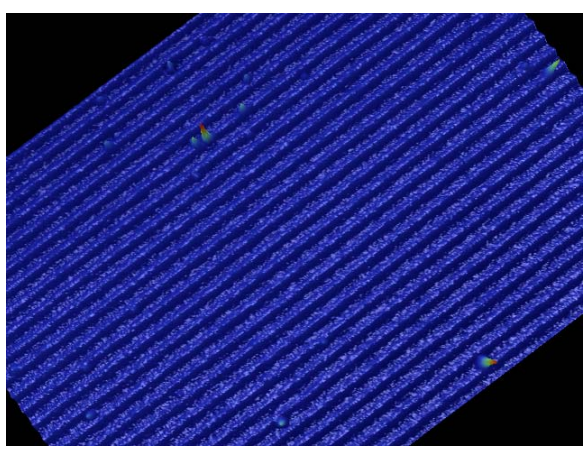

Figure 3.9. An optical noncontact profilometer holographic grating structure with a grating holographic period of 3.33 µm

Figure 3.10 shows the 3-D features of the gratings under three different exposures. At 40 J/cm^2 exposure, the ridges were less pronounced with rounder peak regions. On increasing to 50 J/cm^2 exposure, the depth of the ridges sharpened slightly without any change in the average depth. On further increasing to 75 J/cm^2 exposure, the ridges deepened and were well-defined.

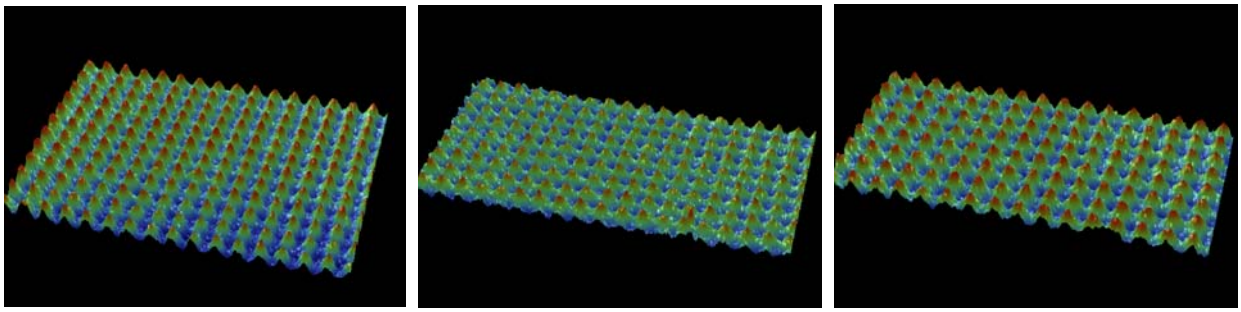

(a) 75 J/cm^2 exposure d = 3.34 microns (b) 50 J/cm^2 exposure d = 3.31 microns (c) 40 J/cm^2 exposure d = 3.31 microns

Figure 3.10. (a) – (c) 3D optical profilometer image from a cross grating structure created with an argon-ion laser using different exposures.

4. CONCLUSIONS

Optimum chemistry and different techniques have shown promise for fabrication and integration of optical components for quantum sensing in MWIR range. Improvements are needed in the areas of 1) purification of constituents, 2) understanding the laser interaction and developing a feed-back control system for laser writing, 3) optimization of wet chemistry for the correct geometry and quality, and 4) tunability of the periods of the grating structure.

ACKNOWLEDGEMENT

We acknowledge programmatic support from DARPA MTO and programmatic guidance and support of LTC John C. Carrano. PNNL is a multi-program national laboratory operated by Battelle Memorial Institute for the United States Department of Energy under Contract DE-AC06-76RLO 1830.

REFERENCES

1. J. Lucas, "Infrared glasses," *Current Opinion in Solid State & Materials Science*, **4** [2], 181-7, 1999.
2. J. A. Savage, S. Nielsen, "Chalcogenide Glasses Transmitting in the Infrared between 1 and 20 µm - A State of the Art Review," *Infrared Physics*, **5**, 195-204, 1965.
3. A. M. Andriesh, O. V. Bolshakov, V. V. Zhitar, A. A. Popesku, "Optical Effects in Thin Film Waveguides of Glassy Arsenic Sulphide," *Journal of Non-Crystalline Solids*, **90** [1-3], 565-568, 1987.
4. J. P. Guo, S. Ramachandran, S. G. Bishop, D. J. Brady, "Characterization of waveguide and grating formation in As_2S_3"; pp. 139-140 in 1994 *IEEE LEOS Annual Meeting, IEEE LEOS Annual Meeting - Proceedings*, Vol. 2. Edited by IEEE Piscataway NJ USA 94CH3371-2, Boston, MA, USA, 1994.
5. J. F. Viens, C. Meneghini, A. Villeneuve, E. J. Knystautas, M. A. Duguay, K. A. Cerqua-Richardson, S. Schwartz, "Neodymium luminescence from ion-implanted As_2S_3 chalcogenide glass waveguides"; pp. 249 in 1997 Conference on Lasers and Electro-Optics, CLEO, Conference Proceedings - *Lasers and Electro-Optics Society Annual Meeting-CLEO*, Vol. 11. Edited by IEEE Piscataway NJ USA 97CH36110, Baltimore, MD, USA, 1997.
6. T. Cardinal, O. M. Efimov, L. B. Glebov, K. C. Richardson, E. Van Stryland, "Waveguide writing in chalcogenide glasses by train of femtosecond laser pulses"; pp. in 1998 *Conference on Lasers and Electro-Optics*, CLEO, Edited by San Francisco, CA, USA, 1998.

7. A. Saliminia, A. Villeneuve, T. V. Galstyan, S. Larochelle, K. Richardson, "Efficient Bragg gratings in single mode planar waveguide of chalcogenide glasses"; pp. in 1998 *International Symposium on Information Theory, CLEO/EUROPE'98*, Edited by Glasgow, Scotland, 1998.
8. M. Saito, M. Takizawa, M. Miyagi, "Optical and Mechanical Properties of Infrared Fibers," *Journal of Lightwave Technology*, **6** [2], 233-239, 1988.
9. M. Saito, M. Takizawa, M. Miyagi, "Infrared optical fibers with vapor-deposited cladding layer," *Journal of Lightwave Technology*, **7** [1], 158-162, 1989.
10. D. J. McEnroe, W. C. LaCourse, "Tensile strengths of Se, As_2S_3, As_2Se_3, and $Ge_{30}As_{15}Se_{55}$ glass fibers," *Journal of the American Ceramic Society*, **72,** 1491-1494, 1989.
11. A. R. Hilton, Sr., "Chalcogenide glass optical fibers"; pp. 34-42 in *Infrared Fiber Optics III,* Proceedings of SPIE - The International Society for Optical Engineering, Edited by International Society for Optical Engineering, Bellingham WA USA. v. 1591, Boston, MA, USA, 1991.
12. D. Lezal, K. Konak, G. Maze, M. Poulain, "Chalcogenide glasses and fibers for CO laser energy delivery"; pp. 126-132 in *Biomedical Optoelectronic Devices and Systems*, Proceedings of SPIE - The International Society for Optical Engineering, Edited by Society of Photo-Optical Instrumentation Engineers Bellingham WA USA. Volume 2084 1994, Budapest, Hung, 1993.
13. J. S. Sanghera, L. E. Busse, I. D. Aggarwal, "Effect of scattering centers on the optical loss of As_2S_3 glass fibers in the infrared," *Journal of Applied Physics*, **75** [10], 4885-4891, 1994.
14. K. Tanaka, N. Toyosawa, H. Hisakuni, "Photoinduced Bragg gratings in As_2S_3 optical fibers," *Optics Letters*, **20** [19], 1976-1978, 1995.
15. M. Li, Y. Liao, R. Chen, K. Yang, "Fabrication and temperature dependence of As_2S_3 fiber long period grating (LPG)," *Proceedings of SPIE* - the International Society for Optical Engineering, 3897, 79-86, 1999.
16. G. G. Devyatykh, E. M. Dianov, V. G. Plotnichenko, A. A. Pushkin, Y. N. Pyrkov, I. V. Skripachev, G. E. Snopatin, M. F. Churbanov, V. S. Shiryaev, "Low loss infrared arsenic chalcogenide glass optical fibers," *Proceedings of SPIE* - the International Society for Optical Engineering. Volume 4083, 229-237, 2000.
17. T. Gotoh, H. Hayakawa, K. Tanaka, "Photoinduced anisotropy in the ion-conducting amorphous semiconductor Ag-As-S," *Journal of Non-Crystalline Solids*, **266**(B), 944-947, 2000.
18. H. Hisakuni, K. Tanaka, "Laser-induced persistent self-focusing in As_2S_3 glass," *Solid State Communications*, **90** [8], 483-486, 1994.
19. H. Hisakuni, K. Tanaka, "Giant photoexpansion in As_2S_3 glass," *Applied Physics Letters*, **65** [23], 2925-2927, 1994.
20. K. Shiramine, H. Hisakuni, K. Tanaka, "Photoinduced Bragg reflector in As_2S_3 glass," *Applied Physics Letters*, **64** [14], 1771-1773, 1994.
21. K. Tanaka, "Light Intensity Dependence of Photodarkening in amorphous As_2S_3 Films," *Thin Solid Films*, **157** [1], 35-41, 1988.
22. K. Tanaka, H. Hisakuni, "Photoinduced phenomena in As_2S_3 glass under sub-bandgap excitation," *Journal of Non-Crystalline Solids*, **198-200** [pt], 714-718, 1996.
23. K. Tanaka, N. Yoshida, "Direct microfabrication of chalcogenide glasses by light and electron-beam exposures," *Diffusion & Defect Data Pt. B: Solid State Phenomena*, **55**, 153-158, 1997.
24. K. Tanaka, K. Ishida, "Photoinduced anisotropic structures in chalcogenide glasses," *Journal of Non-Crystalline Solids*, **227-230** [Pt], 673-676, 1998.
25. M. Asobe, T. Kanamori, K. I. Kubodera, "Ultrafast all-optical switching using highly nonlinear chalcogenide glass fiber," *IEEE Photonics Technology Letters*, **4** [4], 362-365, 1992.
26. M. Asobe, T. Kanamori, K. I. Kubodera, "Applications of highly nonlinear chalcogenide glass fibers in ultrafast all-optical switches," *IEEE Journal of Quantum Electronics*, **29** [8], 2325-2333, 1993.
27. M. Asobe, H. Itoh, T. Miyazawa, T. Kanamori, "Efficient and ultrafast all-optical switching using high Delta n, small core chalcogenide glass fibre," *Electronics Letters*, **29** [22], 1966-1968, 1993.
28. M. Asobe, H. Kobayashi, H. Itoh, T. Kanamori, "Laser-diode-driven ultrafast all-optical switching by using highly nonlinear chalcogenide glass fiber," *Optics Letters*, **18** [13], 1056-1058, 1993.
29. M. Asobe, T. Kanamori, K. Naganuma, H. Itoh, T. Kaino, "Ultrafast and efficient optical Kerr effects in chalcogenide glass fibers and the application in all-optical switching"; pp. in 1994 IEEE *Nonlinear Optics: Materials, Fundamentals and Applications*, Edited by Waikoloa, HI, USA, 1994.
30. M. Asobe, T. Kanamori, K. Naganuma, H. Itoh, T. Kaino, "Third-order nonlinear spectroscopy in As_2S_3 chalcogenide glass fibers," *Journal of Applied Physics*, **77** [11], 5518-5523, 1995.

31. J. Kobelke, J. Kirchhof, K. Schuster, A. Schwuchow, "Effects of Carbon, Hydrocarbon and Hydroxide Impurities on Praseodymium Doped Arsenic Sulfide Based Glasses," *Journal of Non-Crystalline Solids*, **284** [1-3], 123-127, 2001.
32. B. G. Aitken, C. W. Ponader, "Property Extrema in GeAs Sulphide Glasses," Journal *of Non-Crystalline Solids*, **274** [1], 124-130, 2000.
33. T. Cardinal, K. A. Richardson, H. Shim, A. Schulte, R. Beatty, K. Le Foulgoc, C. Meneghini, J. F. Viens, A. Villeneuve, "Non-Linear Optical Properties of Chalcogenide Glasses in the System as-S-Se," Journal *of Non-Crystalline Solids*, **256,** 353-360, 1999.
34. M. N. Kozicki, Y. Khawaja, et al, "As-S/Ag Systems for Integrated Optics," *Sixth International VLSI Multilevel Interconnection Conference*, Santa Clara, CA, USA, IEEE IEEE Service Center Piscataway NY USA., 1989.
35. O. Saliminen, N. Nordman, P. Riihola, A. Ozols, Andris, " Holographic recording and photocontraction of amorphous As2S3 films by 488.0 nm and 514.5 nm laser light illumination," *Optics Communications* **116,** 310-315, 1995.